EXTENDED ABSTRACT

AICHE ANNUAL MEETING 2006

Mediating Fluidic Self-Assembly with Optical Traps

Andrew H. Ewing, Sangtae Kim and Steven T. Wereley
School of Mechanical Engineering, Purdue University
West Lafayette, IN 47907-2088 USA
E-mail: wereley@purdue.edu

The placement of microscopic objects into desired orientations using only fluid phenomena—known as Fluidic self-assembly (FSA) —has proven to be an effective approach for the parallel assembly of complex microsystems from smaller components of dissimilar materials. Fig. 1 illustrates the minimum cost of assembly relative to part size using pick and place robots. FSA is a means to reduce the minimum cost of assembly which leads to improve commercial feasibility of microsystems integration. However, there is an interest in reducing the size of devices that can readily be assembled using FSA. Such advances would make FSA commonplace for nanosystems integration. Nanoscale phenomena that profoundly influence the motion of small particles include Brownian motion, shear induced migration, and electrolytic effects such as electric double layers. Mediating FSA with controllable external force fields offers means to elucidate multi-physics interference issues encountered during nanoscale assembly. Specifically, optical traps, or optical tweezers, can be used to induce forces which guide the FSA process. An investigation of FSA mediated with optical tweezers will be presented. Specifically, the behavior of non-spherical particles trapped in an optical tweezers and the ability to control the orientation and position of non-spherical particles during assembly will be explored. The presentation will include a theoretical description of the behavior of non-spherical particles trapped in an optical tweezers, as well as an experimental study of such behavior.

Before the mediation of FSA with optical traps can occur, the behavior of trapped polyhedra and other non-spherical objects must be well understood. The current research focuses on characterizing this behavior. The experimental apparatus consists of a single-beam gradient force optical trap integrated with an optical microscope and data acquisition system. A Meredith Instruments 20 mW Helium Neon laser (633 nm) is focused to a diffraction limited spot using a 60x (NA 1.0) water immersion objective attached to a Nikon Eclipse TE200 inverted microscope to create the optical trap. A LaVision charge coupled device (CCD) camera is used to collect optical intensity readings of the specimen plane and the DaVis 7 data acquisition and visualization software is used to produce a grey scale image of the trapped specimen at specific intervals. Fig. 2 shows a grayscale image of a microsphere trapped using the system described above.

Measurement of the orientation of the specimen is done using a combination of fluorescent microscopy techniques and image processing and analysis. Each specimen will be coated in fluorescent dye that can be excited to emit a narrow band of light. An epi-fluorescent filter set surrounding the specimen is used to filter the emitted wavelength to improve the signal to noise ratio of the sample image before image processing and analysis is performed.

To process the image, a Gaussian edge detection filter is applied first to the grayscale image to produce an outline of the specimen with well defined boundaries. A linear regression of the pixels that form the outline of the specimen will produce a line-- the slope of which represents the angular displacement of the major axis of the specimen. Angular displacement about the minor axis is a function of the projected area and shape of the specimen and is determined using image analysis algorithms.

A theoretical approximation of the orientation of the specimen is found by solving Eq. (1) for theta, where T_{Opt} is the torque due to the optical forces and T_{Drag} is the toque due to Stoke's drag.

$$I\frac{d^2\theta}{dt^2} = T_{Opt} - T_{Drag} \tag{1}$$

When the wavelength of the incident light is smaller than the characteristic size of the trapped specimen, T_{Opt} can be found by integrating the torque contribution of each ray over the surface of the specimen, as given in Eq. (2) where r is the distance vector from the center of mass to the point at which the force exerted by a ray is applied. The differential force contribution of a ray, dF, is given by Eq. (3) where n_1 is the index of refraction of the surrounding medium and c is the speed of light in a vacuum.

$$T_{Opt} = \int (r \times dF) \tag{2}$$

$$dF = \frac{n_1 R(I \bullet dA)}{c} \tag{3}$$

In Eq. (2) I and dA are the intensity and the area of the incident ray, respectively. R is either the Fresnel reflection or transmission coefficient depending on whether the ray is being reflected or transmitted. This analysis is performed for a rectangular prism and a prolate spheroid. An illustration of a light ray propagating through an ellipsoid and the resultant free body diagram are shown in Fig. 3.

The final presentation should include experimental and theoretical results for the aforementioned investigation.

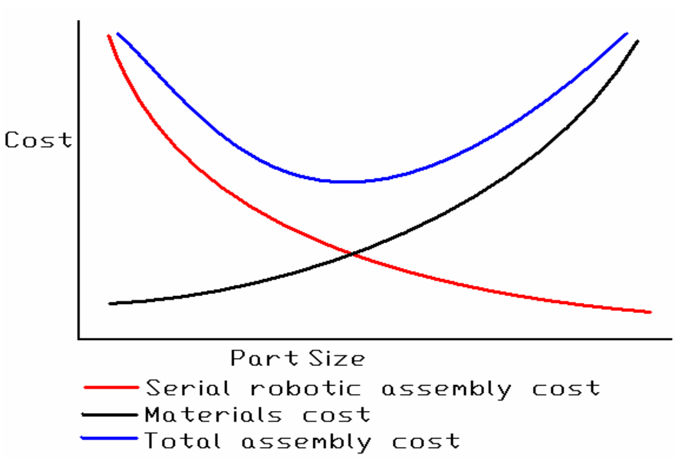

Figure 1: The blue curve represents the total cost of assembly using pick and place robots, whereas the red and black curves are the cost of operating serial assembly robots and the cost of materials, respectively.

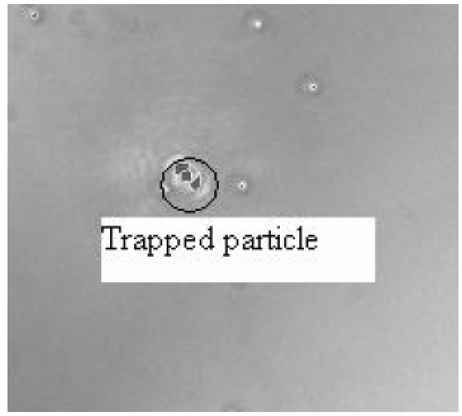

Figure 2: A polystyrene latex microsphere (0.7um diameter) is trapped in an optical tweezers. Astigmatic aberration is visible due to the broadband light used to create the image. Such aberration is not present during the actual experiment. The aberration presented in the image is to show the particle is scattering the incident laser.

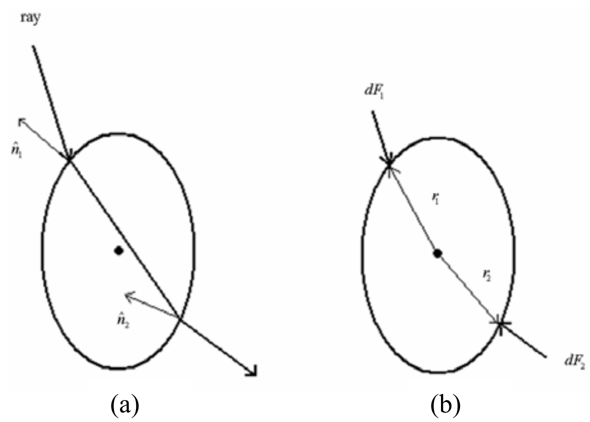

Figure 3: A ray tracing diagram (a) is shown for a single ray propagating through a prolate spheroid with normal vectors $\hat{n}_1$ and $\hat{n}_2$. The free body diagram (b) for such system is shown with differential force contributions dF_1 and dF_2 and moment arms r_1 and r_2.